

Gamma-ray emission from proton-proton interactions in hot accretion flows

Andrzej Niedźwiecki,^{1*} Fu-Guo Xie^{2,3*} and Agnieszka Stępnik^{1*}

¹*Department of Astrophysics, University of Łódź, Pomorska 149/153, 90-236 Łódź, Poland*

²*Key Laboratory for Research in Galaxies and Cosmology, Shanghai Astronomical Observatory, Chinese Academy of Sciences, 80 Nandan Road, Shanghai 200030, China*

³*Kavli Institute for Astronomy and Astrophysics, Peking University, Beijing 100871, China*

30 July 2018

ABSTRACT

We present a model of γ -ray emission through neutral pion production and decay in two-temperature accretion flows around supermassive black holes. We refine previous studies of such a hadronic γ -ray emission by taking into account (1) relativistic effects in the photon transfer and (2) absorption of γ -ray photons in the radiation field of the flow. We use a fully general relativistic description of both the radiative and hydrodynamic processes, which allows us to study the dependence on the black hole spin. The spin value strongly affects the γ -ray emissivity within ~ 10 gravitational radii. The central regions of flows with the total luminosities $L \lesssim 10^{-3}$ of the Eddington luminosity (L_{Edd}) are mostly transparent to photons with energies below 10 GeV, permitting investigation of the effects of space-time metric. For such L , an observational upper limit on the γ -ray (0.1 – 10 GeV) to X-ray (2 – 10 keV) luminosity ratio of $L_{0.1-10\text{GeV}}/L_{2-10\text{keV}} \ll 0.1$ can rule out rapid rotation of the black hole; on the other hand, a measurement of $L_{0.1-10\text{GeV}}/L_{2-10\text{keV}} \sim 0.1$ cannot be regarded as the evidence of rapid rotation, as such a ratio can also result from a flat radial profile of γ -ray emissivity (which would occur for nonthermal acceleration of protons in the whole body of the flow). At $L \gtrsim 10^{-2}L_{\text{Edd}}$, the γ -ray emission from the innermost region is strongly absorbed and the observed γ -rays do not carry information on the value of a . We note that if the X-ray emission observed in Centaurus A comes from an accretion flow, the hadronic γ -ray emission from the flow should contribute significantly to the MeV/GeV emission observed from the core of this object, unless it contains a slowly rotating black hole and protons in the flow are thermal.

Key words: accretion, accretion discs – black hole physics – gamma-rays: theory

1 INTRODUCTION

Early investigations of black hole accretion flows indicated that tenuous flows can develop a two-temperature structure, with proton temperature sufficient to produce a significant γ -ray luminosity above 10 MeV through π^0 production (e.g. Dahlbacka, Chapline & Weaver 1974). The two-temperature structure is an essential feature of the optically-thin, advection dominated accretion flow (ADAF) model, which has been extensively studied and successfully applied to a variety of black hole systems (see, e.g., reviews in Yuan 2007, Narayan & McClintock 2008, Yuan & Narayan 2013) over the past two decades, following the work of Narayan & Yi (1994). Mahadevan, Narayan & Krolik (1997; hereafter M97) pointed out that γ -ray emission resulting from proton-proton collisions in ADAFs

may be a signature allowing to test their fundamental nature. The model of M97 relied on a non-relativistic ADAF model and their computations were improved by Oka & Manmoto (2003; hereafter OM03) who used a fully general relativistic (GR) model of the flow. However, both M97 and OM03 neglected the Doppler and gravitational shifts of energy as well as gravitational focusing and capturing by the black hole, which is a major deficiency because the γ -ray emission is produced very close to the black hole's horizon. Furthermore, both works neglected the internal absorption of γ -ray photons to pair creation, which effect should be important in more luminous systems.

ADAFs are supposed to power low-luminosity AGNs, like Fanaroff-Riley type I (FR I) radio galaxies or low-luminosity Seyfert galaxies, and a measurement, or even upper limits on their γ -ray emission, may put interesting constraints on the properties of the source of high-energy radiation in such objects. M97 and OM03 considered only the *CGRO/EGRET* source in the direction

* E-mail: niedzwiecki@uni.lodz.pl (AN), fgxie@shao.ac.cn (FGX), agastepnik82@gmail.com (AS)

of the Galactic Center for such an analysis. Significant progress in exploration of the γ -ray activity of AGNs which has been made after their works, thanks to the *Fermi* mission, motivates us to develop a more accurate model of the hadronic γ -ray emission from ADAFs. Detections of γ -ray emission from objects with misaligned jets (e.g. Abdo et al. 2010b) are most relevant for our study. Their γ -ray radiation is usually explained as a jet emission; we show that emission from an accretion flow may be a reasonable alternative, at least in some FR Is. We focus on modelling of radiation in 100 MeV – 10 GeV energy range, relevant for the *Fermi*-LAT measurements of the FR I radio galaxies (Abdo et al. 2010b) and over which the upper limits in Seyfert galaxies are derived (Ackermann et al. 2012).

The dependence of the γ -ray luminosity on the black hole spin parameter makes a particularly interesting context for such an investigation. Already a rough estimate by Shapiro, Lightman & Eardley (1976) indicated a strong dependence of the γ -ray luminosity from a two-temperature flow on the spin of the black hole and, then, they suggested that this effect may serve as a means to measure the spin value (see also Eilek & Kafatos 1983 and Colpi, Maraschi & Treves 1986). OM03, who made GR calculations for the modern ADAF model, found a dramatic dependence of the γ -ray luminosity on the spin value in models with thermal distribution of proton energies, however, they concluded that the dependence is weak if protons have a nonthermal distribution. In this work we extend the analysis of this issue and clarify some related properties.

We find global solutions of the hydrodynamical ADAF model, which follows Manmoto (2000), and use them to compute the γ -ray emission. Similarly to M97 and OM03 we take into account emission resulting from thermal and nonthermal distribution of proton energies; we use similar phenomenological models, with some modifications which allow to illustrate separately effects due to local distribution of proton energies and to radial profile of γ -ray emissivity. We also use our recently developed model of global Comptonization (Niedźwiecki, Xie & Zdziarski 2012; hereafter N12, see also Xie et al. 2010) to compute the X-ray emission, which allows to investigate the internal absorption of γ -ray photons to pair creation in the flow.

In our computations we assume a rather weak magnetic field, with the magnetic pressure of 1/10th of the total pressure, supported by results of the magnetohydrodynamic (MHD) simulations in which amplification of magnetic fields by the magneto-rotational instability typically saturates at such a ratio of the magnetic to the total pressure (e.g. Machida, Nakamura & Matsumoto 2004, Hirose et al. 2004, Hawley & Krolik 2001). We investigate the dependence on the poorly understood parameter in ADAF theory, δ , describing the fraction of the turbulent dissipation that directly heats electrons in the flow. We take into account only one value of the accretion rate, but the considered ranges of the spin and δ parameters yield a rather large range of bolometric luminosities of $\sim 10^{-4}$ to 10^{-2} of the Eddington luminosity. In our paper we present both the spectra affected by $\gamma\gamma$ absorption and those neglecting the absorption effect; the latter may be easily scaled to smaller accretion rates, for which the $\gamma\gamma$ absorption becomes unimportant.

2 HOT FLOW MODEL

We consider a black hole, characterised by its mass, M , and angular momentum, J , surrounded by a geometrically thick accretion flow with an accretion rate, \dot{M} . We define the following dimensionless parameters: $r = R/R_g$, $a = J/(cR_g M)$, $\dot{m} = \dot{M}/\dot{M}_{\text{Edd}}$,

where $\dot{M}_{\text{Edd}} = L_{\text{Edd}}/c^2$, $R_g = GM/c^2$ is the gravitational radius and $L_{\text{Edd}} \equiv 4\pi GMm_p c/\sigma_T$ is the Eddington luminosity. Most results presented in this work correspond to $M = 2 \times 10^8 M_\odot$, in Fig 5a we present also results for $M = 2 \times 10^6 M_\odot$. We consider $\dot{m} = 0.1$ and three values of the spin parameter, $a = 0, 0.95$ and 0.998 . The inclination angle of the line of sight to the symmetry axis is given by θ_{obs} . We assume that the density distribution is given by $\rho(R, z) = \rho(R, 0) \exp(-z^2/2H^2)$, where H is the scale height at r . We assume the viscosity parameter of $\alpha = 0.3$ and the ratio of the gas pressure (electron and ion) to the total pressure of $\beta_B = 0.9$. The fraction of the dissipated energy which heats directly electrons is denoted by δ .

Our calculations of hadronic processes are based on global solutions of the fully GR hydrodynamical model of two-temperature ADAFs, described in N12, which follows closely the model of Manmoto (2000). Here we recall only the ion energy equation, which is most important for the present study:

$$0 = (1 - \delta)Q_{\text{vis}} + Q_{\text{compr}} - \Lambda_{\text{ie}} - Q_{\text{int}}, \quad (1)$$

where Λ_{ie} is the Coulomb rate, the compressive heating and the advection of the internal energy of ions, respectively, are given by

$$Q_{\text{compr}} = -\frac{\dot{M} p_i}{2\pi R \rho} \frac{d \ln \rho}{dR}, \quad Q_{\text{int}} = -\frac{\dot{M} p_i}{2\pi R \rho (\Gamma_i - 1)} \frac{d \ln T_i}{dR}, \quad (2)$$

and the viscous dissipation rate, per unit area, is given by

$$Q_{\text{vis}} = -\alpha p H (2\pi)^{1/2} \frac{\gamma_\phi^4 A^2}{r^7} \frac{d\Omega}{dr}, \quad (3)$$

where $p = (p_i + p_e)/\beta_B$, p_i is the ion pressure, p_e is the electron pressure, Γ_i is the ion adiabatic index, Ω is the angular velocity of the flow, γ_ϕ is the Lorentz factor of the azimuthal motion and $A = r^4 + r^2 a^2 + 2ra$. The form of the energy equation given in equation (1) is standard in ADAFs theory, although actually it should include an additional term describing the direct cooling of protons to pion production, Q_γ . In our calculation of hadronic processes we find that Q_γ is approximately equal to Λ_{ie} at $r < 10$. At $\dot{m} = 0.1$, considered in this work, both Q_γ and Λ_{ie} are much smaller, by over 3 orders of magnitude, than the effective heating $Q_{\text{vis}} + Q_{\text{compr}}$ and the heating is fully balanced by the advective term, Q_{int} . This justifies our neglect of the direct hadronic cooling.

The only difference between our GR model and that of Manmoto (2000) involves the simplifying assumption of $d \ln(R)/d \ln(H) = 1$ adopted in the latter; we do not follow this simplification and an exact $H(R)$ profile is considered in all our hydrodynamic equations. We note that the simplification has a considerable effect in the central part of the flow, e.g. it results in an underestimation of the proton temperature by a factor of ~ 1.5 within the innermost $10R_g$. Applying the above simplifying assumption we get exactly the same flow parameters as Manmoto (2000); note, however, that Manmoto (2000) assumed an equipartition between the gas and plasma pressures, with $\beta_B = 0.5$, which in general gives a smaller proton temperature than $\beta_B = 0.9$ assumed here. In particular, for $a = 0$ and $\delta = 10^{-3}$, models with $\beta_B = 0.9$ give the proton temperature larger by a factor of ≈ 4 , close to the horizon, than models with $\beta_B = 0.5$. This underlies also the differences in the γ -ray luminosity levels between the thermal models of Oka & Manmoto (2003) and ours, as discussed in Section 3.

To obtain global transonic solutions we have to adjust the specific angular momentum per unit mass accreted by the black hole, for which the accretion flow passes smoothly through the sonic point, r_s . We note that this condition permits for two kinds of solutions, below referred to as a 'standard' and a 'superhot' solution.

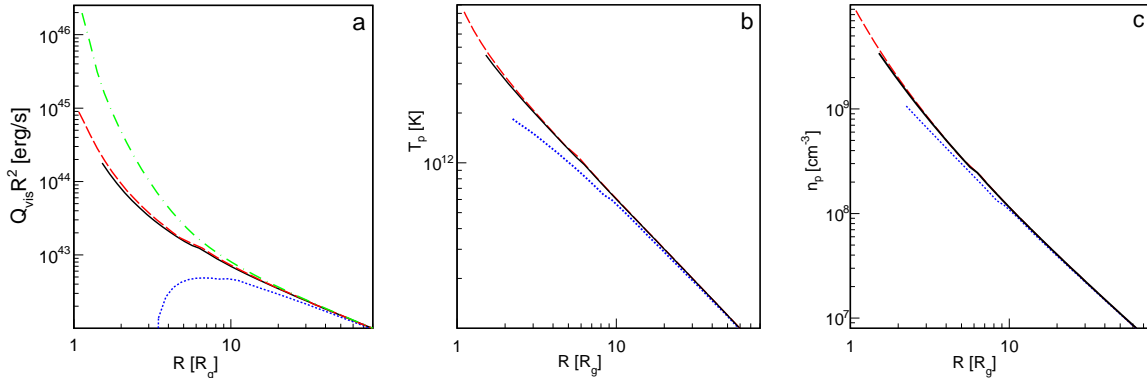


Figure 1. Radial profiles of the dissipative heating rates, Q_{vis} (a), the proton temperature (b) and the proton number density (c) of our hot-flow solutions for $\delta = 10^{-3}$. In all panels, the dashed (red) lines are for $a = 0.998$, the solid (black) lines are for $a = 0.95$ and the dotted (blue) lines are for $a = 0$. In panel (a), Q_{vis} denotes a vertically integrated rate, so $Q_{\text{vis}}R^2$ gives the heating rate (per unit volume) times volume. The green (dashed) line in panel (a) shows Q_{vis} in the superhot solution (see text) for $a = 0.998$. $M = 2 \times 10^8 M_{\odot}$, $\dot{m} = 0.1$, $\alpha = 0.3$ and $\beta_{\text{B}} = 0.9$ in this and all further figures in this paper.

The latter (superhot) has much larger proton temperature and density, furthermore, the sound speed is large and the sonic point located in the immediate vicinity of the event horizon, e.g. $r_s \approx 1.2$ for $a = 0.998$. In the standard solutions the sonic point is located at larger distances, $r_s > 2$. Taking into account rather extreme properties of the superhot solutions (specifically, a very large magnitude of Q_{vis} illustrated in Fig. 1(a) and discussed in Section 6.1) we neglect them in this work and for all values of a we consider only the standard solutions which are consistent with solutions of the model investigated in several previous studies (e.g. Manmoto 2000, Yuan et al 2009, Li et al. 2009). Note, however, that in our previous works (N12, Niedźwiecki, Xie & Beckmann 2012) we considered the superhot solution with $a = 0.998$, then, the results for $a = 0.998$ discussed in those works correspond to flows with larger proton temperature and density (both by a factor of ~ 5) than these considered in the present study.

Fig. 1 shows the dependence on the black hole spin of some parameters from our solutions which are crucial for the hadronic γ -ray production. Rotation of the black hole stabilizes the circular motion of the flow which yields a higher density (through the continuity equation). Furthermore, the stabilized rotation of the flow results in a stronger dissipative heating giving a larger proton temperature for larger a . All these differences are significant only within the innermost $\sim 10R_{\text{g}}$.

3 HADRONIC γ -RAY EMISSION AND RELATIVISTIC TRANSFER EFFECTS

The hydrodynamical solutions set the proton density, n_p , and temperature, T_p , as a function of radius. In principle, this should allow to determine the γ -ray emissivity, resulting from neutral pion production in proton-proton collisions and their subsequent decay into γ -ray photons, in the rest frame of the flow. However, details of this process are subject to an uncertainty related to the distribution of proton energies, which is unlikely to be thermal in optically thin flows (see discussion in Section 6.2). Following M97 and OM03 we assume that the temperature from the global solution functions as a parameter specifying the average energy of protons in the plasma which, however, does not have to have a thermal distribution. We consider several phenomenological models which must satisfy the obvious requirements that at each radius (1) the number density of

protons equals $n_p(r)$, determined by the global ADAF solution and (2) the average energy of protons equals the average energy

$$U_{\text{th}}(\theta_p) = \theta_p m_p c^2 (6 + 15\theta_p) / (4 + 5\theta_p). \quad (4)$$

of the Maxwellian proton gas with temperature, $T_p(r)$, determined by the global ADAF solution, where $\theta_p = kT_p / m_p c^2$ and we use the simplified (cf. Gammie & Popham 1998) relativistic form of $U_{\text{th}}(\theta_p)$.

We consider models involving various combinations of thermal

$$n_{\text{th}}(\gamma) = n_{\text{th}} \gamma^2 \beta \exp(-\gamma/\theta_p) / [\theta_p K_2(1/\theta_p)], \quad (5)$$

and power-law

$$n_{\text{pl}}(\gamma) = n_{\text{pl}}(s-1)\gamma^{-s}, \quad (6)$$

distributions of proton energies, where n_{th} and n_{pl} are the local densities of these two populations. The thermal model (model T) assuming a purely Maxwellian distribution of protons and the non-thermal model (model N, same to nonthermal models of M97 and OM03), assuming that the total energy is stored in the power-law distribution of a small fraction of protons, allow us to estimate the *minimum* and *maximum* level of γ -ray luminosity, respectively, for a given set of $(M, \dot{m}, a, \alpha, \beta, \delta)$. Mahadevan (1999) and OM03 considered the model involving the mixture of the thermal and power-law distributions, with the radius-independent parameter characterizing the fraction of energy that goes into the two distributions. Deviations of such a model from model N are trivial, with the γ -ray luminosity linearly proportional to the fraction of energy going to the power-law distribution. In this work we consider a different hybrid model (model H) with the radius dependent normalization between the power-law and the thermal distribution, which allows us to illustrate some additional effects.

The detailed assumptions on the parameters of these models are as follows ($n_p(r)$ and $T_p(r)$ denote values given by the global ADAF solution):

Model T assumes a purely Maxwellian distribution of protons, equation (5), with $n_{\text{th}} = n_p(r)$ and $\theta_p = kT_p(r) / m_p c^2$.

Model N assumes that a fraction ψ of protons form the power-law distribution, equation (6), with the radius-independent index s and $n_{\text{pl}} = \psi(r)n_p(r)$, and the remaining protons are cold, with the Lorentz factor $\gamma \approx 1$ ($\gamma = 1$ is assumed in the computations). The radius-dependent fraction ψ is determined by

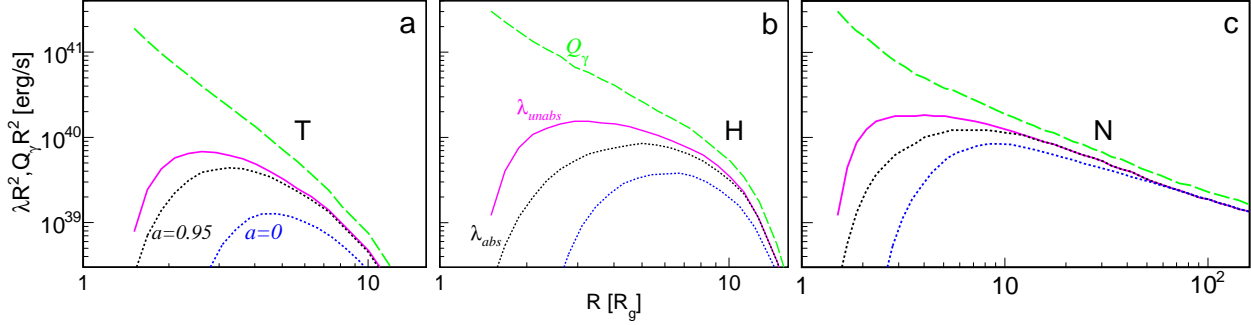


Figure 2. Dashed (green) lines show the radial profiles of the vertically-integrated γ -ray emissivities, Q_γ , for models with $a = 0.95$. Solid (magenta) lines show the local contribution to the luminosity at infinity from a unit area of the flow neglecting the $\gamma\gamma$ absorption, λ_{unabs} , for $a = 0.95$. The dotted lines show the local contribution to the luminosity at infinity from a unit area of the flow taking into account the $\gamma\gamma$ absorption, λ_{abs} , for $a = 0.95$ (upper, black) and $a = 0$ (lower, blue). (a) model T; (b) model H with $s = 2.6$; (c) model N with $s = 2.6$. All models assume $\delta = 10^{-3}$.

$$\frac{\psi m_p c^2}{s-2} = U_{\text{th}} [T_p(r)]. \quad (7)$$

Model H assumes that an efficient nonthermal acceleration operates only within the central $\sim 15R_g$, where the average proton energies resulting from the ADAF solutions become relativistic. Specifically, we assume that at each radius at $r < 15$ a fraction of protons form a thermal distribution at a subrelativistic temperature of $T = 4.3 \times 10^{11}$ K ($\theta_p = 0.04$), and the remaining form a power-law distribution (equation 6) with a constant (i.e. radius-independent) index s and $n_{\text{pl}} = \psi(r)n_p(r)$. The relative normalization of these two distributions is determined by

$$\frac{\psi m_p c^2}{s-2} + (1-\psi) \frac{6.6}{4.2} m_p c^2 = U_{\text{th}} [T_p(r)], \quad (8)$$

(where the factor $6.6/4.2$ results from equation (4) with $\theta_p = 0.04$). At $r > 15$, where $T_p < 4.3 \times 10^{11}$ K, there are no non-thermal protons in this model, which then results in a negligible pion production at such distances, similar as in model T. The chosen value of $T = 4.3 \times 10^{11}$ K gives a smooth transition between a purely thermal and a hybrid plasma at $r = 15$, however, radiative properties of model H are roughly independent of the specific value of the temperature of the subrelativistic thermal component. We remark also that $T = 4.3 \times 10^{11}$ K is close to the limiting temperature above which the pion production prevents thermalization of protons (see Stepney 1983, Dermer 1986b)

The efficiency of pion production by protons with the power-law distribution increases with the decrease of the power-law index s . On the other hand, the fraction ψ decreases with decreasing s , roughly as $\psi \propto (s-2)$. These two effects balance each other yielding the largest luminosity in 0.1–10 GeV range, $L_{0.1-10\text{GeV}}$, for $s \simeq 2.5-2.6$. For $2.3 < s < 2.8$, the dependence of $L_{0.1-10\text{GeV}}$ on s is weak; for $s = 2.1$, $L_{0.1-10\text{GeV}}$ is by a factor of ~ 2 smaller than for $s = 2.6$. To estimate the maximum value of $L_{0.1-10\text{GeV}}$ that can be produced in a flow with given parameters, in our computations for models N and H we use $s = 2.6$. For all values of a , $\theta_p > 0.1$, and also $\psi > 0.1$ in models H and N with $s = 2.6$, within the innermost several R_g .

In our solutions of the flow structure we assume that protons are thermal and we use the thermal form of the gas pressure. Then, our models N and H with non-thermal proton distributions are not strictly self-consistent, as their pressure may deviate from the thermal prescription. However, this is a rather small effect, e.g. the pressure of the purely non-thermal distribution (model N) differs by 20–30 per cent from the pressure of a thermal gas with the same internal energy.

For a given distribution of proton energies we determine the γ -ray spectra in the flow rest frame, strictly following Dermer (1986a, 1986b), in a manner similar to M97 and OM03; however, we do not apply the following simplification underlying their non-thermal model. As argued in M97, the fraction of nonthermal protons should be small, $\psi \ll 1$, and, therefore, interactions of non-thermal protons with other nonthermal protons may be neglected; hence, only interaction of nonthermal protons with cold protons are taken into account in their computations. We remark that such an approach underestimates the γ -ray luminosity, e.g. by a factor of ~ 2 in model N with $a = 0.95$ and $s = 2.6$ (for which $\psi \simeq 0.4$ in the innermost region). In all our models we take into account interaction of protons with all other protons.

To compute the γ -ray luminosity and spectra received by distant observers we use a Monte Carlo method similar to that described in Niedźwiecki (2005). We generate γ -ray photons isotropically in the plasma frame, make a Lorentz transformation from the flow rest frame to the locally non rotating (LNR) frame and then we compute the transfer of γ -ray photons in curved space-time; see, e.g., Bardeen et al. (1972) for the definition of LNR frames and the equations of motion in the Kerr metric.

The dashed lines in Fig. 2 show the radial profiles of the vertically-integrated γ -ray emissivity, Q_γ (Q_γ gives the energy emitted from the unit area per unit time) for models T, H and N with $a = 0.95$. The solid lines in Fig. 2 show the radial profiles of the vertically-integrated local luminosity (the energy per unit time reaching infinity from the unit area at a given r). The local luminosity profiles shown by the solid lines neglect the $\gamma\gamma$ absorption, so the difference between the dashed and solid lines is only due to the relativistic transfer effects. Fig. 3 shows the corresponding γ -ray spectra and compares them with the spectra for $a = 0$. At $r < 10$ both models N and H are characterised by similar values of ψ and produce similar amounts of γ -rays. In both models T and H the contribution from $r > 10$ is very weak; in model N the radial emissivity is much flatter despite ψ being small, e.g. $\psi < 5 \times 10^{-3}$ at $r > 100$. Comparing models T and H we can see the effect of the local proton distribution function and by comparing models H and N we can see the effect of the radial emissivity.

For the thermal distribution of protons, the rest-frame photon spectra are symmetrical, in the logarithmic scale, around ~ 70 MeV but in EF_E units they peak around 200 MeV; the position of the maximum in the spectra observed by distant observers is slightly redshifted. Note that the difference of γ -ray luminosities, L_γ , between $a = 0$ and 0.95 in our model T is much smaller than that

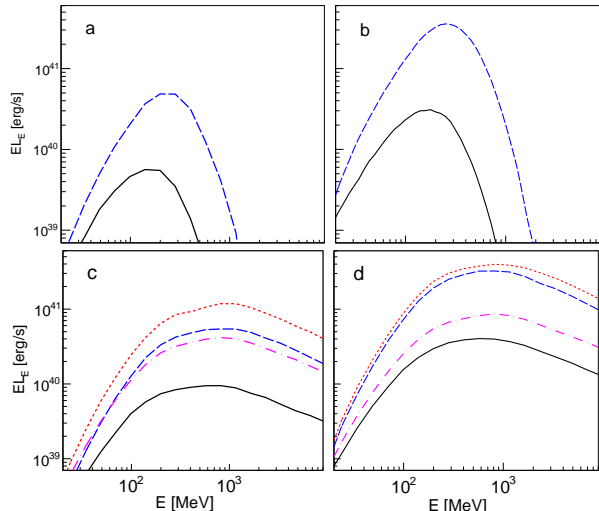


Figure 3. Dashed (blue) and solid (black) lines show the rest frame and the observed γ -ray spectra, respectively, for model T (ab) and model H with $s = 2.6$ (cd). Dotted (red) and dot-dashed (magenta) lines in (cd) show the rest frame and the observed γ -ray spectra, respectively, for model N with $s = 2.6$. All spectra are for $\delta = 10^{-3}$; panels (a) and (c) are for $a = 0$, panels (b) and (d) are for $a = 0.95$. In this figure, the observed spectra neglect $\gamma\gamma$ absorption, so they are affected only by GR effects.

derived by OM03, whose thermal models with $a = 0$ and 0.95 give L_γ differing by approximately three orders of magnitude. The difference is due to different values of β_B assumed here and by OM03, which result in different θ_p , as discussed in Section 2. The dependence of L_γ on θ_p changes around $\theta_p \approx 0.1$ (see, e.g., fig. 3 in Dermer 1986b). At lower temperatures, L_γ is extremely sensitive to θ_p , with the increase of θ_p by a factor of 2 yielding the increase of L_γ by over two orders of magnitude. At $\theta_p > 0.1$, the dependence is more modest, e.g. the increase of θ_p from 0.2 to 0.4 results in the increase of L_γ by only a factor of ~ 2 . For $\beta_B = 0.9$ assumed in this work, $\theta_p > 0.1$ at small r for all values of a , making the γ -ray luminosity much less dependent on the black hole spin. For $\beta_B = 0.5$, assumed by OM03, the proton temperature is small, with the maximum value of $\theta_p \approx 0.03$ for $a = 0$, which leads to the strong dependence of L_γ on a .

For both model H and N, the spectrum at $E > 1$ GeV has the same slope as the power-law distribution of proton energies. For model H with $s = 2.6$, L_γ is by a factor of 3 larger than in model T. Rather small difference between L_γ in our thermal and nonthermal models is again due to our assumption of a weak magnetic field. At smaller β_B , resulting in smaller θ_p , the presence of even a small fraction of non-thermal electrons leads to the increase of L_γ by orders of magnitude, as can be seen by comparing the emissivities of our models N and T at $r > 10$ (see also M97).

For models T and H the bulk of the γ -ray emission comes from $r < 10$ (Fig. 2ab) and the GR transfer effects reduce the detected γ -ray flux by approximately an order of magnitude. In model N the magnitude of the GR effects on the total flux is reduced due to strong contribution from $r > 10$ (which is weakly affected by GR). Also in model N, the contribution from $r > 10$, which for $a = 0$ approximately equals the contribution from $r < 10$, reduces the difference between the γ -ray fluxes observed for $a = 0$ and $a = 0.95$ to only a factor of ~ 2 , see Fig. 3(cd).

The viewing-angle dependent spectra for model H, which would be observed (if unabsorbed) by distant observers, are shown by the dashed and dotted lines in Fig. 4. The flows considered in

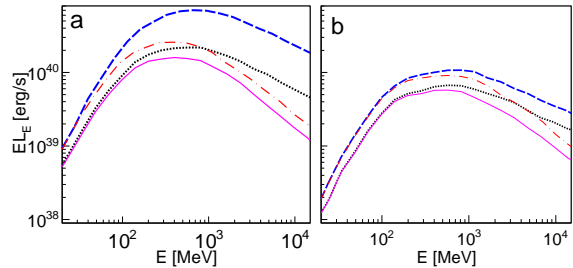


Figure 4. Observation-angle dependent γ -ray spectra taking into account and neglecting the $\gamma\gamma$ absorption for model H with $s = 2.6$; $a = 0.998$ (a) and $a = 0$ (b). The dot-dashed (red) and dashed (blue) lines show the spectra observed at $\theta_{\text{obs}} = 70^\circ$, with and without absorption, and the solid (magenta) and dotted (black) lines show the spectra observed at $\theta_{\text{obs}} = 30^\circ$, with and without absorption, respectively.

this work are quasi-spherical and optically thin and hence their appearance depends on the viewing angle primarily due to the relativistic transfer effects. Most importantly, trajectories of photons emitted close to a rapidly rotating black hole are bent toward its equatorial plane. Therefore, the γ -ray radiation has a significant intrinsic anisotropy in models with large a , with edge-on directions corresponding to larger γ -ray fluxes.

4 COMPTONIZATION AND $\gamma\gamma$ ABSORPTION

The absorption of γ -rays in the radiation field of the flow has been calculated in a fully GR model by Li et al. (2009). Here we use a similar approach with the major difference involving the computation of target photon density. Li et al. (2009) considered the propagation of photons with energies of 10 TeV, which are absorbed mostly in interactions with infra-red photons. Those low energy photons are produced primarily by the synchrotron emission which can be simply modelled using its local emissivity. In turn, photons with energies in 0.1–10 GeV range, considered in this work, are mostly absorbed by the UV and soft X-ray photons, which are produced by Comptonization. Then, an exact computation of the angular-, energy- and location-dependent distribution of the target photon field requires the precise modelling of the Comptonization taking into account its global nature. In our model we apply the Monte Carlo (MC) method, described in detail in N12, with seed photons for Comptonization from synchrotron and bremsstrahlung emission.

We find self-consistent electron temperature distributions using the procedure described in N12; we iterate between the solutions of the electron energy equation (analogous to equations 1–3; note that here we include the direct electron heating, while N12 assumes $\delta = 0$) and the GR MC Comptonization simulations until we find mutually consistent solutions. In Fig. 5 we show the resulting spectra. Fig. 6 shows the radial profiles of the radiative cooling of electrons (strongly dominated by Comptonization), Q_{Compt} , for $\delta = 10^{-3}$ and compares them with the γ -ray emissivity, Q_γ , for model T. Note that Q_γ is much steeper than Q_{Compt} so the GR effects are more important for the γ -ray than for the X-ray emission.

As we can see in Fig. 6 and also in the corresponding spectra in Fig. 5a, for $\delta = 10^{-3}$ the black hole spin negligibly affects the Comptonized radiation; this property results from a large magnitude of the compression work, which is roughly independent of a and dominates the heating of electrons for small values of δ (cf. N12).

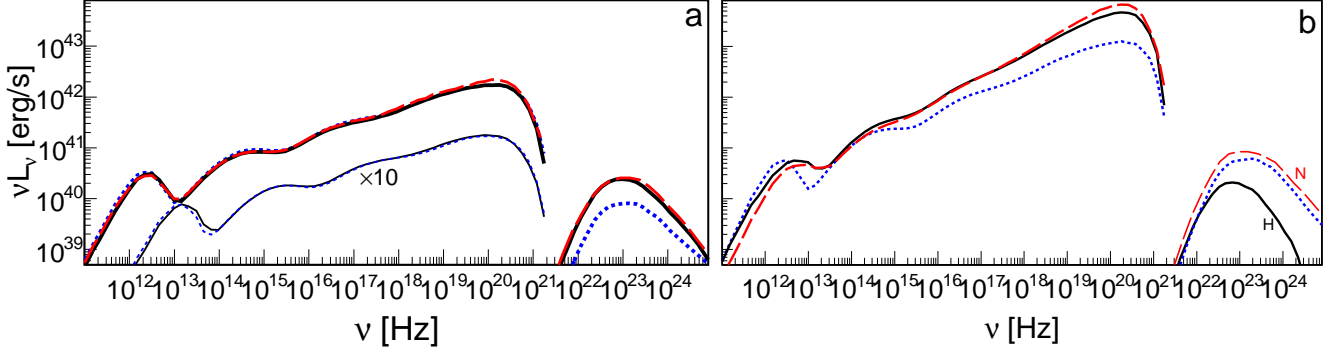


Figure 5. Angle-averaged spectra received by a distant observer; the synchrotron and Comptonized (radio to X-rays) and hadronic (γ -rays) components are shown separately. In both panels $a = 0.998$ (dashed, red), 0.95 (solid, black) and 0 (dotted, blue) (a) Models with $\delta = 10^{-3}$; the γ -ray spectra correspond to model H with $s = 2.6$. (b) Models with $\delta = 0.5$; the γ -ray spectra correspond to model N with $s = 2.6$ for $a = 0$ and 0.998 and to model H with $s = 2.6$ for $a = 0.95$. The lower pair of lines in panel (a), rescaled by a factor of 10, show the spectra (leptonic component) for $M = 2 \times 10^6 M_{\odot}$.

For $\delta \geq 0.1$ the direct heating contributes significantly to the heating of electrons and for $\delta = 0.5$ it dominates over other heating processes at $r < 100$ for all values of a . Then, the dependence of Q_{vis} on a results in a noticeable dependence of the Comptonized radiation on a for $\delta \geq 0.1$ (see also Xie & Yuan 2012 for a recent study of the dependence of X-ray luminosity on δ). The radiative efficiency increases from $\eta = 0.004$ for all values of a at $\delta = 10^{-3}$ to $\eta = 0.02$ for $a = 0$, $\eta = 0.08$ for $a = 0.95$ and $\eta = 0.1$ for $a = 0.998$ at $\delta = 0.5$. Despite considering only one value of accretion rate, our solutions span a range of bolometric luminosities, from $L \approx 4 \times 10^{-4} L_{\text{Edd}}$ (for $\delta = 10^{-3}$) to $L \approx 10^{-2} L_{\text{Edd}}$ (for $\delta = 0.5$ and $a = 0.998$). The corresponding X-ray spectral slopes harden from $\Gamma_X \approx 1.7$ to $\Gamma_X \approx 1.5$ with the increase of L . Note that these values correspond to the range of parameters close to the turning point in the L - Γ correlation observed in AGNs (e.g. Gu & Cao 2009). Then, we likely consider here the range of the largest luminosities of the flows in which synchrotron emission is the dominant source of seed photons for Comptonization (see discussion and references in N12).

Having found the self-consistent solutions, described above, we apply our MC model to tabulate the distribution of all photons propagating in the central region (up to $r_{\text{out}} = 1000$), $dn_{\text{ph}}(R, \theta, E_{\text{LN}}, \Omega_{\text{LN}})/dE_{\text{LN}} d\Omega_{\text{LN}}$ (in photons $\text{cm}^{-3} \text{eV}^{-1} \text{sr}^{-1}$), where R and θ are the Boyer-Lindquist coordinates, E_{LN} is the photon energy in the LNR frame and $d\Omega_{\text{LN}}$ is the solid angle element in the LNR frame.

To compute the optical depth to pair creation, $\tau_{\gamma\gamma}$, we closely follow the method for determining an optical depth to Compton scattering in the Kerr metric, see Niedźwiecki (2005) and Niedźwiecki & Zdziarski (2006), however, here we calculate the probability of pair creation in the LNR frame whereas for the Compton effect an additional boost to the flow rest frame is applied. While Compton scattering is most conveniently described in the plasma rest frame, pair production can be simply modelled in the LNR frame and, thus, the transformation to the flow rest frame is not necessary here. We solve equations of the photon motion in the Kerr metric and we determine the increase of the optical depth along the photon trajectory from

$$d\tau_{\gamma\gamma} = \int \int \int (1 - \cos \theta_{\text{LN}}) \sigma_{\gamma\gamma} \frac{dn_{\text{ph}}}{dE_{\text{LN}} d\Omega_{\text{LN}}} dE_{\text{LN}} d\Omega_{\text{LN}} dl_{\text{LN}}, \quad (9)$$

where dl_{LN} is the length element in the LNR frame, $\sigma_{\gamma\gamma}(E_{\text{LN}}, E_{\gamma\text{LN}}, \theta_{\text{LN}})$ is the pair production cross section (e.g., Gould & Schreder 1967), $E_{\gamma\text{LN}}$ is the energy of the γ -ray photon

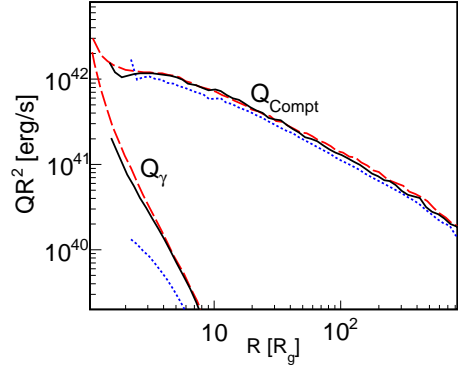


Figure 6. Radial profiles of the γ -ray emissivity, Q_{γ} (for model T), and the Comptonization rate Q_{Compt} , for $a = 0.998$ (dashed, red), 0.95 (solid, black) and 0 (dotted, blue) in models with $\delta = 10^{-3}$. Q denotes the vertically integrated rates.

in the LNR frame and θ_{LN} is the angle between the interacting photons in the LNR frame.

GR affects the $\gamma\gamma$ opacity through (1) bending the trajectories of both the γ -ray photon and target photons and (2) changing energies of both the γ -ray photon and target photons. As an example, the neglect of the gravitational shift of the γ -ray photon energy, by using $\sigma_{\gamma\gamma}(E_{\text{LN}}, E_{\gamma}, \theta_{\text{LN}})$ (where E_{γ} is the energy at infinity) instead of $\sigma_{\gamma\gamma}(E_{\text{LN}}, E_{\gamma\text{LN}}, \theta_{\text{LN}})$ in equation (9), underestimates $\tau_{\gamma\gamma}$ by a factor of ≈ 2 –3 for photons emitted from the innermost region.

In Fig. 7 we show values of the total optical depth, $\tau_{\gamma\gamma}(r)$, integrated along the outward radial direction in the equatorial plane from the emission point at the radial coordinate r to the outer boundary at r_{out} . As we can see, the $\gamma\gamma$ opacity is a strong function of both the γ -ray energy and the location in the flow. The dotted lines in Fig. 2 show how the $\gamma\gamma$ absorption attenuates γ -rays observed from a given r .

It is apparent that around $\dot{m} \sim 0.1$ flows undergo transition from being fully transparent to mostly opaque to γ -rays. In our models with the Eddington ratio $L/L_{\text{Edd}} = 4 \times 10^{-4}$, the flow is fully transparent to photons with energies $\lesssim 100$ MeV; at higher energies the absorption leads to moderate attenuation, with the increase of the photon index at $E > 1$ GeV by $\Delta\Gamma \approx 0.2$, see Fig. 4. The size of the γ -ray photosphere (the surface of $\tau_{\gamma\gamma} = 1$) increases with increasing L and for $L \approx 10^{-2} L_{\text{Edd}}$ the GeV photons cannot escape from $r < 10$. At such L , our model H gives spectra with

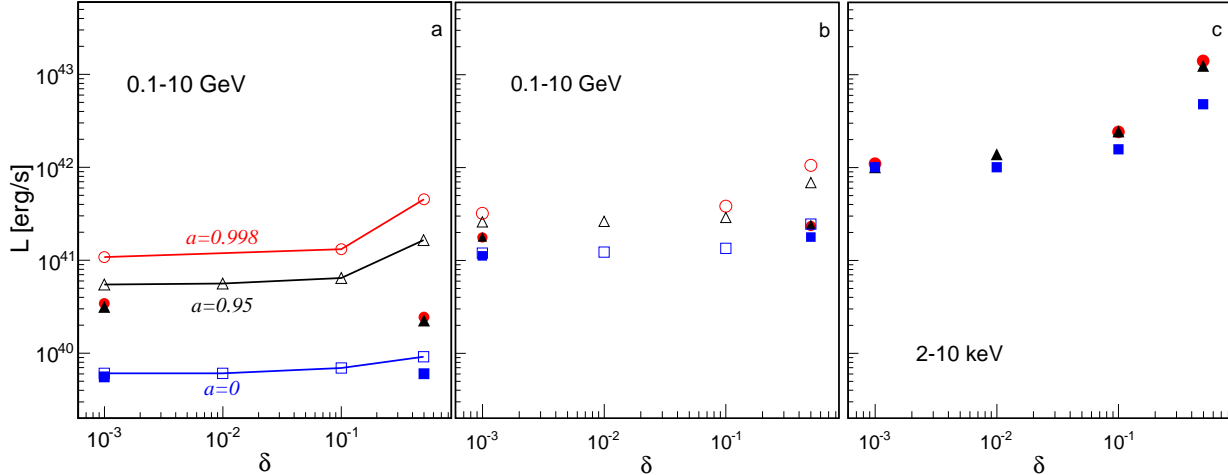


Figure 8. Observed, angle-averaged γ -ray luminosity in 0.1–10 GeV range in model T (a) and model N with $s = 2.6$ (b) and X-ray luminosity in the 2–10 keV range (c) as a function of δ for $a = 0.998$ (circles), $a = 0.95$ (triangles) and $a = 0$ (squares). The filled symbols in (ab) show $L_{0.1-10\text{GeV}}$ after the $\gamma\gamma$ absorption, the open symbols show the luminosity L_{unabs} neglecting the absorption.

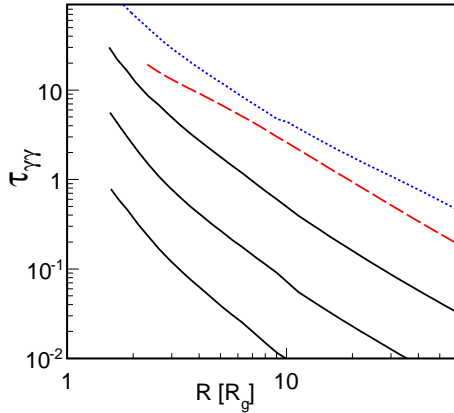


Figure 7. The optical depth to pair creation for radially outgoing γ -ray photons with $E_\gamma = 100$ MeV, 1 GeV and 10 GeV from bottom to top, as a function of the radial distance of their point of emission for $a = 0.95$ and $\delta = 10^{-3}$ are shown by the solid (black) lines. The dotted (blue) and dashed (red) lines are for $a = 0.95$ and 0 in models $\delta = 0.5$; in these models $\tau_{\gamma\gamma}$ is shown only for $E = 10$ GeV for clarity.

a clear cut-off around 1 GeV (see the solid line in Fig. 5b) which could be measured by *Fermi*. In other cases absorption leads to a smooth softening of the spectra.

In terms of the 2–10 keV luminosity, $L_{2-10\text{keV}}$, flows with $L_{2-10\text{keV}} < 10^{-5} L_{\text{Edd}}$ should be fully transparent to MeV/GeV photons. Flows with $L_{2-10\text{keV}} > 10^{-3} L_{\text{Edd}}$ can emit significant amounts of unabsorbed γ -rays only if their γ -ray emissivities are strong at large r . E.g. in our model N, the luminosity of the flow at $r > 50$, which region would be outside the photosphere of 1 GeV photons even at much larger $L_{2-10\text{keV}} \sim 10^{-2} L_{\text{Edd}}$, is $L_{0.1-10\text{GeV}} \approx 10^{40}$ erg/s. Then, the γ -ray luminosity exceeding 10^{41} erg/s can be expected at $m > 0.3$ if the γ -ray emitting flow extends out to several tens of R_g , which property is, however, unclear as objects with high luminosities often show signs of a cold disc extending to rather small radii (so the transition between the hot and cold flow may occur within the γ -ray photosphere). Note that for such a scenario, with γ -ray emission from a hot flow at large L , we expect a small luminosity ratio of $L_{0.1-10\text{GeV}}/L_{2-10\text{keV}} \sim 10^{-3}$ regardless of the value of a .

5 X-RAY VS γ -RAY LUMINOSITY

In Fig. 8 we summarize our results regarding the relation between the X-ray and γ -ray luminosities. The range of expected $L_{0.1-10\text{GeV}}$ is constrained from below by values indicated in Fig. 8a for model T, and from above by values in Fig. 8b for model N. As we can see, the models give the luminosity ratios $L_{0.1-10\text{GeV}}/L_{2-10\text{keV}}$ between ~ 0.002 and 0.2.

In model T, $L_{0.1-10\text{GeV}}$ for $a = 0$ and $a = 0.998$ differ by a factor of several; the unabsorbed luminosities differ by over an order of magnitude but for L close to $10^{-2} L_{\text{Edd}}$ the $\gamma\gamma$ absorption reduces the difference to a factor of ~ 4 . In model N, $L_{0.1-10\text{GeV}}$ for $a = 0$ and $a = 0.998$ differ by only a factor of ~ 2 ; as noted before, the difference is reduced here due to contribution from large r . Model N for $a = 0$ gives similar $L_{0.1-10\text{GeV}}$ as model T with large a ; larger density and average energy for large a is approximately compensated by a larger fraction of protons above the pion production threshold for model N. Note, however, that - despite similar luminosities - the spectra for these two regimes differ significantly, see Fig. 3.

In model H, $L_{0.1-10\text{GeV}}$ has a similar dependence on a as in model T, with a large difference between small and high values of a . We conclude that it is the radial distribution of γ -ray emissivity, rather than the local proton distribution, which reduces the dependence on a . This is even more hindering for attempts of assessing the spin value basing on the γ -ray luminosity level. The proton energy distribution function is reflected in the produced spectral shape and, therefore, it could be constrained observationally and taken into account in this kind of analysis. On the other hand, one cannot expect to derive information on the radial emissivity profile from observations, so an investigation of black hole spin values using the γ -ray luminosity should be subject to significant uncertainty.

In models with a dominant contribution from the central $\sim 10R_g$, intrinsic γ -ray luminosities of flows around submaximally ($a = 0.95$) and maximally ($a = 0.998$) rotating black holes differ by a factor of ~ 2 . For the latter, the flow extends to smaller radii and hence a larger proton temperature and density are achieved, see Fig. 1. However, a strong contribution from $r > 10$ as well as $\gamma\gamma$ absorption make the difference between the observed luminosities insignificant.

Regarding the dependence on δ , we notice a somewhat sur-

prising property of models with $\delta = 0.5$, which predict a larger γ -ray luminosity than models with smaller δ (the effect is more pronounced for larger values of a). The physical reason is that for $\delta = 0.5$, the slight decrease of proton temperature is outweighed by the increase of density (through the decrease of both the radial velocity and the scale height with decreasing temperature), cf. Mamoto (2000), which leads to the increase of $L_\gamma \propto n_p^2 T_p$. At smaller values of δ , the intrinsic L_γ depends negligibly on δ , in agreement with the results of OM03 for $a = 0$ and $\delta \leq 0.3$ in their nonthermal model.

The scaling of density with \dot{m} and M in our global GR solutions only weakly differs from that of self-similar ADAF model, i.e. $n \propto \dot{m}/M$ (e.g. Mahadevan 1997). Then, the intrinsic γ -ray luminosity can be estimated as $L_{0.1-10\text{GeV}} \simeq L_{\text{unabs}}(\dot{m}/0.1)^2(M/2 \times 10^8 M_\odot)^{-1}$ erg/s, where L_{unabs} is the unabsorbed luminosity shown by the open symbols in Fig. 8(ab). This gives also the observed luminosity at $\dot{m} < 0.1$, when the absorption effects are unimportant. Obviously, the above scaling with \dot{m} is not relevant for $\dot{m} \gtrsim 0.1$, for which the increase of \dot{m} results in the decrease of the observed $L_{0.1-10\text{GeV}}$ due to $\gamma\gamma$ absorption. On the other hand, the linear scaling of the γ -ray luminosity with M holds even when the $\gamma\gamma$ absorption is important. The spectral distribution of Comptonized radiation changes slightly with the black hole mass (due to the change of the synchrotron emission, which affects the position of Comptonization bumps, see Fig 5a), however, the effect is insignificant for the $\gamma\gamma$ opacity and we have checked that it negligibly affects the observed γ -ray spectra.

6 DISCUSSION

The form of the dissipation rate and the proton distribution function are two major uncertainties for predicting the γ -luminosity. We briefly discuss here the related effects in accretion flows.

6.1 Viscous heating

The form of the viscous dissipation rate given by equation (1) results from the usual assumption that the viscous stress is proportional to the total pressure, with the proportionality coefficient α . We use this form of the viscous stress for computational simplicity, however, as we discuss in N12, this may be an oversimplified approach (although it has support in MHD simulations, see below). Below we briefly compare the dissipation rate in our models with that predicted by the classical Novikov & Thorne (1973) model. We define Q_{vis} integrated over the whole body of the flow as the total dissipation rate, $Q_{\text{vis,tot}}$, in our solutions and compare it to the dissipation rate in a Keplerian disc for the corresponding value of a , $Q_{\text{NT,tot}}$, given by the Novikov & Thorne model. Obviously, $Q_{\text{vis,tot}}$ does not need to match $Q_{\text{NT,tot}}$ closely. The latter value is calculated under the assumption that the shear stress vanishes at the radius of the innermost stable circular orbit (ISCO), which condition is not applicable to geometrically thick ADAFs and its release should lead to stronger dissipation. On the other hand, ADAFs are sub-Keplerian which property decreases the dissipation rate.

Our $Q_{\text{vis,tot}}$ does not differ significantly from $Q_{\text{NT,tot}}$, however, the efficiency of dissipation in our model comparatively increases with increasing a . Specifically, $Q_{\text{vis,tot}} = 0.025\dot{M}c^2 \approx 0.5Q_{\text{NT,tot}}$ for $a = 0$, $Q_{\text{vis,tot}} = 0.2\dot{M}c^2 \approx Q_{\text{NT,tot}}$ for $a = 0.95$ and $Q_{\text{vis,tot}} = 0.58\dot{M}c^2 \approx 1.5Q_{\text{NT,tot}}$ for $a = 0.998$. Note that in an ADAF with a large value of a most of the dissipation occurs very deep in the

potential, where relativistic effects strongly reduce the energy escaping to infinity, whereas in a Keplerian disc the dissipation is less centrally concentrated and its radiation is subject to less severe reduction. For example, the gravitational redshift alone (neglecting, e.g., the photon capture under the event horizon) would give similar luminosities received by distant observers ($\approx 0.3\dot{M}c^2$) both in our ADAF and in Novikov & Thorne models with $a = 0.998$, if all of the dissipated energy were converted into radiation. Obviously, in optically thin ADAFs only a small part of the dissipated energy is radiated away and most of it is accreted by the black hole, so the radiative efficiency is much smaller than 0.3.

As we mentioned in Section 2, the model formally allows for two solutions and the above values of $Q_{\text{vis,tot}}$ correspond to the standard solution, considered in previous sections. The superhot solution has an extreme dissipation, with $Q_{\text{vis,tot}} \approx 5-10\dot{M}c^2$. This is not necessarily an unphysical property (note that $Q_{\text{vis,tot}}$ is defined in the rest frame of the flow), as the observed luminosity of such flows does not exceed the accretion rate of the rest mass energy. Nevertheless, the magnitude of Q_{vis} suggests that the underlying assumption of $Q_{\text{vis}} \propto p$ breaks down at very large p .

The issue of the proper description of the Q_{vis} term could be partially resolved by comparing analytic models such as our, aiming at a precise calculation of the produced radiation, with MHD simulations. The latter currently neglect radiative cooling, or use very approximate descriptions for it, in turn, they provide more accurate accounts of the dissipation physics. Such MHD simulations support some properties of our model, e.g. the $Q_{\text{vis}} \propto p$ prescription of viscous heating (Ohsuga et al. 2009). Furthermore, the GR MHD simulations have shown that flows cross the ISCO without any evidence that the shear stress goes to zero, which leads to the increase of the radiative efficiency, and the deviations from Novikov & Thorne model increase with increasing H/R ratio (e.g. Noble, Krolik & Hawley 2009, Penna et al. 2010). We could not, however, quantitatively compare our models with such simulations, as the published results have a much smaller aspect ratio than our solutions ($H/R > 0.5$).

Lastly, we remark that Gammie & Popham (1998) and Popham & Gammie (1998) present a model similar to ours but with a more elaborate description of the shear stress (in turn, they neglect radiative processes). We note that their results indicate a similar in magnitude stabilizing effect of the rotation of black hole.

6.2 Proton distribution function

As pointed out by Mahadevan & Quataert (1998), Coulomb collisions are too inefficient to thermalize protons in optically thin flows and the proton distribution function is determined by the viscous heating mechanism, which is poorly understood. Our solutions, with $M = 2 \times 10^8 M_\odot$ and $\dot{m} = 0.1$, give the accretion time-scale, t_a , much shorter than the proton relaxation time-scale, t_{pp} ; e.g. at $r \leq 20$, $t_a < 10$ hours and $t_{pp} > 10^5$ hours. Clearly, the protons cannot redistribute their energy through Coulomb collisions.

In solar flares, the best observationally studied example of particle acceleration/heating in a magnetised plasma, a significant fraction of the released energy is carried by non-thermal, high energy particles (e.g. Aschwanden 2002), which strongly motivates for considering the nonthermal distribution of protons, as originally proposed in M97. Applying the generic description of particle acceleration, see e.g. section 3 in Zdziarski, Malzac & Bednarek (2009), we check whether the conditions in ADAFs allow for proton acceleration to ultrarelativistic energies, as assumed in our computations for the power-law distributions. The magnetic field

strength in our ADAF solutions is $B \simeq 10$ G, 100 G and 1000 G at $r = 100$, 10 and 2, respectively. Assuming an acceleration rate $dE/dt \propto \xi eB$, where e is the elementary charge and ξ is the acceleration efficiency ($\xi \lesssim 1$), we find that the maximum Lorentz factor limited by the synchrotron energy loss is $\gamma_{\max} \sim 10^6 - 10^7$, depending on r . Another condition, of the Larmor radius being smaller than the acceleration site size, R_{acc} , gives $\gamma_{\max} \sim 10^7$ at $r \gg 100$, and larger values of γ_{\max} at smaller r , even if we safely assume $R_{\text{acc}} = 1R_g (= 3 \times 10^{13}$ cm). We conclude that the central region of a hot accretion flow may be a site of the acceleration of protons to energies which easily allow hadronic emission of photons even in the TeV range. This conclusion remains valid for the whole relevant range of accretion rates and masses of supermassive black holes, as the strength of the magnetic field scales as $B \propto \dot{m}^{1/2} M^{-1/2}$.

Considering processes which could compete with proton-proton interactions, we note that proton-photon interactions are much less efficient in the central region of the flow. Namely, the number density of γ -ray photons, which can effectively interact with protons in photomeson production, is by a factor of $\sim 10^3$ smaller than the number density of protons within the innermost few R_g ; the number density of hard X-ray photons, which can interact with protons in photopair production, is similar to n_p . The cross-section for both channels of proton-photon interactions is by over two orders of magnitude smaller than the cross-section for proton-proton interaction, making the photo-hadronic production of secondary particles negligible.

7 COMPARISON WITH OBSERVATIONS

We briefly compare here predictions of our model with γ -ray observations of objects which may be powered by ADAFs. We note, however, that for a more detailed comparison additional physical processes, related to charged pion production (cf. Mahadevan 1999), should be taken into account. In particular, relativistic electrons produced by the pion decay should be important in modelling the emission in the MeV range. We also tentatively discuss the origin in the accretion flow of the very high energy radiation detected from M87 and Sgr A*, for the latter under assumption that the contributions from two separate sources dominate above 100 GeV (Sgr A*) and at lower energies (diffuse emission) in the radiation observed from the Galactic Center region. However, we note that the opacity at very high energies may be affected by the nonthermal synchrotron emission of the relativistic electrons. The work on the model implementing the effects of charged pions is currently in progress.

7.1 Misaligned AGNs

The misaligned AGNs detected by the *Fermi*-LAT include seven FR I radio galaxies and four FR IIs (Abdo et al. 2010b). The low-power FR I galaxies are supposed to be powered by radiatively inefficient accretion flows (e.g. Balmaverde, Baldi & Capetti 2008) and, thus, are more relevant for application of our results. Interestingly, Wu, Cao & Wang (2011) assess that supermassive black holes in FR Is rotate rapidly, with $a > 0.9$. The X-ray emission of more luminous FR Is is supposed to come from an accretion flow (e.g. Wu, Yuan & Cao 2007), but their γ -ray emission tends to be interpreted in terms of jet emission (e.g. Abdo et al. 2009, 2010ab). FR Is are supposed to be the parent population of BL Lac objects, however, the Lorentz factors required by a jet model are much lower than typical values found in models of BL Lac objects (see, e.g., Abdo

et al. 2010b). Therefore, the radiation observed in FR Is and BL Lacs must have a different origin, which adds some complexity to the jet model for FR Is. At least two FR I galaxies reported in Abdo et al. (2010b), M87 and Centaurus A, are detected because of their proximity rather than a small inclination angle of their jets and, then, they are interesting targets for searching for the γ -ray emission from accretion flows.

In Niedźwiecki et al. (2012a) we roughly compared preliminary results of our model with the X/ γ -ray observational data of Centaurus A from *INTEGRAL* and *Fermi*-LAT. We found that the ADAF model, which matches the X-ray emission in this object, predicts the γ -ray emission significantly weaker than measured by *Fermi* if the value of the spin parameter a is small. We should emend, however, that this conclusion is valid only for models assuming a significant γ -ray emission only from the central $\sim 10R_g$, such as our models T and H. Regardless of the values of a and δ , our model N with $s = 2.6$ predicts the absorbed $L_{0.1-10\text{GeV}}$ approximately consistent with 1.3×10^{41} erg/s measured in Cen A by *Fermi* (Abdo et al. 2010a). Also regardless of the value of a , our models with $\delta = 10^{-3}$ predict the 2-10 keV flux as well as the X-ray spectral index consistent with that observed in Cen A; for $\delta \gtrsim 0.1$ the model overpredicts the flux and hardness of the X-ray radiation. In the above we assumed the black hole mass of $2 \times 10^8 M_\odot$ (e.g. Marconi et al. 2001), which is also within the range allowed by the recent measurement of Gnerucci et al. (2011).

The central core of the accretion system in M87 has been considered as the γ -ray emitting region e.g. by Neronov & Aharonian (2007) in their model with particle acceleration in the black hole magnetosphere. The accretion rate assessed from the high-resolution observations of the nucleus of M87 by *Chandra*, and used to model the multiwavelength spectrum of the nucleus by emission from an ADAF, by Di Matteo et al. (2003; note that their definition of \dot{m} differs from ours by a factor of 10), $\simeq 0.1 M_\odot/\text{year}$, corresponds to $\dot{m} \simeq 0.01$ for a black hole with $M = 3 \times 10^9 M_\odot$. At such \dot{m} the central region should be transparent to γ -ray photons. Then, we compare the unabsorbed luminosities from our non-thermal models with $s = 2.2$ (approximately consistent with the slope of the *Fermi* data above 200 MeV; Abdo et al. 2009) and $M = 3 \times 10^9 M_\odot$ with the γ -ray measurements of M87. We find that the luminosity derived in the 0.2-10 GeV range by *Fermi* (Abdo et al. 2009), and above 100 GeV by ground-based telescopes (e.g. Aleksić et al. 2012) in the low state of M87, can be reproduced by our model with $a = 0.998$ and $\simeq 0.14 M_\odot/\text{year}$ (for $\theta_{\text{obs}} = 40^\circ$). The required accretion rate, larger by 40 per cent than the face value of the estimate in Di Matteo et al. (2003), is allowed by the precision of the estimation of the accretion rate using Bondi accretion theory. We conclude that hadronic processes in ADAF can contribute significantly to the γ -ray emission observed in M87 in the low state, or even explain these observations entirely. However, such a model requires that all the available material forms the innermost flow, i.e. it does not allow a strong reduction the accretion rate in the central region by outflows (assumed in models of Sgr A*, see below).

7.2 Sgr A*

The value of \dot{m} in the central region is the major issue for applications of ADAF models to the supermassive black hole in the Galactic Center. The Bondi accretion rate corresponds to $\dot{m}_B \simeq 10^{-3}$ for $M \simeq 3 \times 10^6 M_\odot$ and early models used such \dot{m} to explain the broadband spectra of Sgr A* (e.g. Narayan et al. 1998). The measurement of the millimetre/submillimetre polarization of Sgr A* is often assumed to limit the accretion rate to $\dot{m} \leq 3 \times 10^{-5}$ (e.g. Marrone et al.

2007), but counterarguments are presented, e.g., by Mościbrodzka, Das & Czerny (2006) and Ballantyne, Özel & Psaltis (2007). An updated ADAF model to Sgr A*, with $\dot{m} \approx 10^{-5}$ and strong electron heating, is presented in Yuan, Quataert & Narayan (2003). An alternative to ADAF model, proposed by Mościbrodzka et al. (2006) and recently applied by Okuda & Molteni (2012), with the low angular momentum flow, assumes $\dot{m} \approx 6 \times 10^{-4}$. The low angular momentum flow has a similar density in the innermost region as an ADAF with the same \dot{m} , but much smaller proton temperature $< 4 \times 10^{11}$ K. Then, the magnitude of hadronic processes could be used to distinguish the two classes of models; however, the low T may be an artificial effect resulting from the neglect of viscosity in the former (low angular momentum) class.

The *CGRO*/EGRET source, 3EG J1746-2851, was initially considered as a possible γ -ray counterpart of Sgr A*; Narayan et al. (1998) and OM03 found that their ADAF models underpredicted the γ -ray luminosity implied by the EGRET measurement. However, improved analyses (e.g. Pohl 2005) subsequently indicated that 3EG J1746-2851 is displaced from the exact Galactic Center and excluded Sgr A*, as well as the TeV source observed with HESS which may be directly related with Sgr A*, as its possible counterparts.

Recently, Chernyakova et al. (2011) analysed the *Fermi*-LAT observations of the Galactic Center and combined them with the HESS observational data of the point-like source (Aharonian et al. 2009). The spectrum of the source seen in the MeV/GeV band by *Fermi* is consistent with a π^0 -decay spectrum. The HESS data indicate flattening of the spectrum above 100 GeV, suggesting that at the highest energies a different spectral component dominates, with rather hard spectrum, $\Gamma \approx 2.2$. In the EF_E plot, the normalization of the HESS source is an order of magnitude larger than the quiescent X-ray emission of Sgr A*. To explain these observations, Chernyakova et al. (2011) discuss a model, following previous works (e.g. Atayan & Dermer 2004), with protons accelerated in the accretion flow and then diffusing outwards to interact with dense gas at distances of ~ 1 pc. The emission at energies below 100 GeV may be explained by interactions of protons injected into the interstellar medium during a strong flare of Sgr A* that occurred 300 years ago, as protons generating photons with such energies are still diffusively trapped in the γ -ray production region. On the other hand, most of the higher energy protons have already escaped and hence an additional, persistent injection of high-energy protons has to be assumed to account for the HESS observations, with the required rate of 2×10^{39} erg/s implying a very high efficiency of the conversion of the accreting rest mass energy into the proton energy.

We remark that alternatively the spectral component above 100 GeV can be explained by proton-proton interactions in an accretion flow around a rapidly rotating black hole. Our model with $a = 0.998$, $s = 2.2$ and edge-on viewing direction predict the flux consistent with the HESS detection for $\dot{m} = 3 \times 10^{-4}$. The scenario with the γ -ray emission produced in the accretion flow may be tested over the following years, if the fall of the gas cloud into the accretion zone of Sgr A* (Gillessen et al. 2012) results in the increase of the mass accretion rate.

7.3 Seyfert galaxies

Spectral properties of the Seyfert galaxy, NGC 4151, are consistent with the model of an inner hot flow surrounded by an outer cold disc (e.g. Lubiński et al. 2010), however, its rather large luminosity, $L > 0.01 L_{\text{Edd}}$ indicates that a potential γ -ray emission from innermost region would be strongly absorbed. The constraint of

$L_{0.1-10\text{GeV}}/L_{14-195\text{keV}} < 0.0025$ derived for this object in Ackermann et al. (2012) can still give interesting information if the spectral model constrains the parameters of the inner hot/outer cold accretion system (in particular, the distance of transition between the two modes of accretion). The constraint of $L_{0.1-10\text{GeV}}/L_{14-195\text{keV}} < 0.1$, or even < 0.01 for some objects, found for other Seyfert galaxies by Ackermann et al. (2012) is not strongly constraining for the spin value, as can be seen in Fig. 8 (note that $L_{14-195\text{keV}}$ is by a factor of a few, depending on Γ_X , larger than $L_{2-10\text{keV}}$), especially for large X-ray luminosities (and hence strong $\gamma\gamma$ absorption) characterising most of objects analysed in that paper.

8 SUMMARY

We have studied the γ -ray emission resulting from proton-proton interactions in two-temperature ADAFs. Our model relies on the global solutions of the GR hydrodynamical model, same as OM03, but we improve their computations by taking into account the relativistic transfer effects as well as the $\gamma\gamma$ absorption and by properly describing the global Comptonization process.

We have found that the spin value is reflected in the properties of γ -ray emission, but the effect is not thrilling. The speed of the black hole rotation strongly affects the γ -ray emission produced within the innermost $10R_g$. If emission from that region dominates, the observed γ -ray radiation depends on the spin parameter noticeably; the intrinsic γ -ray luminosities of flows around rapidly-rotating and non-rotating black holes differ by over a factor of ~ 10 . However, if the γ -ray emitting region extends to larger distances, the dependence is reduced. In the most extreme case with protons efficiently accelerated to relativistic energies in the whole body of the flow, the regions within and beyond $10R_g$ give comparable contributions to the total emission, reducing the difference of γ -ray luminosities between high and low values of a to only a factor of ~ 2 . The radial emissivity profile of γ -rays is very uncertain (as the acceleration efficiency may change with radius), then, the level of the γ -ray luminosity cannot be regarded as a very sensitive probe of the spin value. Still, it may be possible to assess a slow rotation in a low luminosity object by putting an upper limit on the γ -ray luminosity at the level of $\lesssim 0.01$ of the X-ray luminosity. The presence of nonthermal protons may be easily assessed from the γ -ray spectrum as for a purely thermal plasma the total γ -ray emission would be observed only at energies lower than 1 GeV.

We have considered the accretion rate of $\dot{m} = 0.1$, for which our model gives the bolometric luminosities between $\approx 4 \times 10^{-4} L_{\text{Edd}}$ and $10^{-2} L_{\text{Edd}}$. Such \dot{m} , with the corresponding range of L/L_{Edd} , seems to be favoured for investigation of the hadronic γ -ray emission, with the related effects of the space-time metric, because the internal γ -ray emission is large and its attenuation by $\gamma\gamma$ absorption is weak. Flows with $L > 10^{-2} L_{\text{Edd}}$ can produce observable γ -ray radiation only if the emitting region extends out to a rather large distance of several tens of R_g .

We have found the X-ray to γ -ray luminosities ratio as a function of the black hole spin and the efficiency of the direct heating of electrons. The $L_{0.1-10\text{GeV}}/L_{2-10\text{keV}}$ ratios reaching ~ 0.1 , with the corresponding levels of the γ -ray luminosities which may be probed in nearby AGNs at the current sensitivity of *Fermi*-LAT surveys, encourage to consider contribution from an accretion flow to the γ -ray emission observed in low-luminosity objects. We point out that such a contribution should be strong at least in Cen A.

The γ -ray luminosity decreases rapidly ($\propto \dot{m}^2$) with decreasing \dot{m} . M87 and Sgr A* are the obvious, however possibly also

unique, objects for which the γ -ray emission from the flow can be searched at $\dot{m} \ll 0.1$. Obviously, contribution from other γ -ray emitting sites should be properly subtracted to establish the luminosity of an accretion flow, which may be particularly difficult in Sgr A*. The ADAF model with a hard (acceleration index $s \simeq 2.2$) nonthermal proton distribution can explain the γ -ray detections of both Sgr A* (above 100 GeV) and M87, however, it does not allow for strong reduction of the accretion rate by outflows. Nevertheless, it seems intriguing that in both nearby, low accretion-rate objects, in which the γ -ray radiation is not suppressed by $\gamma\gamma$ absorption, observations reveal very high energy components, consistent with predictions of such a model. In both objects the model requires a large black hole spin.

The luminosity ratio should decrease rather slowly ($L_\gamma/L_X \propto \dot{m}^{0.3}$, as the radiative efficiency of hot flows varies as $\dot{m}^{0.7}$ at small \dot{m} ; cf. Xie & Yuan 2012) with decreasing \dot{m} . The presence of the γ -ray signal in low-luminosity AGNs is often considered as the evidence for the origin of their radiation in a jet (see, e.g., Takami 2011). We note that such a diagnostic is not valid because accretion flows may produce a similarly strong γ -ray emission as jets in such objects.

ACKNOWLEDGMENTS

We are grateful to Włodek Bednarek for helpful discussions and to the referee for a very careful review and comments which helped us to improve the presentation of the results. This research has been supported in part by the Polish NCN grant N N203 582240. FGX has been supported in part by the NSFC (grants 11103059, 11121062, 11133005, and 11203057), the NBRPC (973 Program 2009CB824800), and SHAO key project No. ZDB201204.

REFERENCES

- Abdo A. A., et al., 2009, *ApJ*, 707, 55
 Abdo A. A., et al., 2010a, *ApJ*, 719, 1433
 Abdo A. A., et al., 2010b, *ApJ*, 720, 912
 Ackermann M., et al., 2012, *ApJ*, 747, 104
 Aharonian F., et al., 2008, *A&A*, 492, L25
 Aharonian F., et al., 2009, *A&A*, 503, 817
 Aleksić, J., et al., 2012, *A&A*, 544, 96
 Aschwanden M. J., 2002, *SSRv*, 101, 1
 Atayan A., Dermer C. D., 2004, *ApJ*, 617, L123
 Ballantyne D. R., Özel F., Psaltis D., 2007, *ApJ*, 663, L17
 Balmaverde B., Baldi R. D., Capetti A., 2008, *A&A*, 486, 119
 Bardeen J. M., Press, W. H., & Teukolsky, S. A., 1972, *ApJ*, 178, 347
 Chernyakova M., Malyshev D., Aharonian F. A., Crocker R. M., Jones D. I., 2011, *ApJ*, 726, 60
 Colpi M., Maraschi L., Treves A., 1986, *ApJ*, 311, 150
 Dahlbacka G. H., Chapline G. F. and Weaver T. A., 1974, *Nature*, 250, 36
 Davis S. W., Laor A., 2011, *ApJ*, 728, 98
 Dermer C. D., 1986a, *A&A*, 157, 223
 Dermer C. D., 1986b, *ApJ*, 307, 47
 Di Matteo T., Allen S. W., Fabian A. C., Wilson A. S., Young A. J. 2003, *ApJ*, 582, 133
 Eilek J. A., Kafatos M., 1983, *ApJ*, 271, 804
 Gammie C. F., 1999, *ApJ*, 522, L57
 Gammie C. F., Popham R., 1998, *ApJ*, 498, 313
 Gammie C. F., Shapiro S. L., McKinney J. C., 2004, *ApJ*, 602, 312G
 Gillissen S., et al., 2012, *Nature*, 481, 51
 Gnerucci A., Marconi A., Capetti A., Axon D. J., Robinson A., Neumayer N., 2011, *AA*, 536A, 86
 Gould R. J., Schröder G. P. 1967, *PhRv*, 155, 1404
 Gu M., Cao X., 2009, *MNRAS*, 399, 349
 Hawley J. F., Krolik J. H., 2001, *ApJ*, 548, 348
 Hirose S., Krolik J. H., De Villiers J. P., Hawley J. F., 2004, *ApJ*, 606, 1083
 Li Y.-R., Yuan Y.-F., Wang J.-M., Wang J.-C., Zhang S., 2009, *ApJ*, 699, 513
 Lubiński P., Zdziarski A. A., Walter R., Paltani S., Beckmann V., Soldi S., Ferrigno C., Courvoisier T. J.-L., 2010, *MNRAS*, 408, 1851
 Machida M., Nakamura K., Matsumoto R., 2004, *PASJ*, 56, 671
 Mahadevan R., 1997, *ApJ*, 477, 585
 Mahadevan R., 1999, *MNRAS*, 304, 501
 Mahadevan R., Quataert E., 1997, *ApJ*, 490, 605
 Mahadevan R., Narayan R., Krolik J., 1997, *ApJ*, 486, 268 (M97)
 Manmoto T., 2000, *ApJ*, 534, 734
 Marconi A., Capetti A., Axon D. J., Koekemoer A., Macchetto D., Schreier E. J., 2001, *ApJ*, 549, 915
 Marrone D. P., Moran J. M., Zhao J.-H., Rao R., 2007, *ApJ*, 654, L57
 Mościbrodzka M., Das T. K., Czerny B., 2006, *MNRAS*, 370, 219
 Narayan R., McClintock, J. E. 2008, *New Astronomy Review*, 51, 733
 Narayan R., Yi I., 1994, *ApJ*, 428, L13
 Narayan R., Mahadevan R., Grindlay J. E., Popham R. G., Gammie C., 1998, *ApJ*, 492, 554
 Neronov A., Aharonian F. A., 2007, *ApJ*, 671, 85
 Niedźwiecki A., 2005, *MNRAS*, 356, 913
 Niedźwiecki A., Zdziarski A. A., 2006, *MNRAS*, 365, 606
 Niedźwiecki A., Xie F.-G., Beckmann V., 2012, *Journal of Physics: Conference Series*, 355, 012035
 Niedźwiecki A., Xie F.-G., Zdziarski A. A., 2012, *MNRAS*, 420, 1195 (N12)
 Noble S. C., Krolik J. H., Hawley J. F., 2009, *ApJ*, 692, 411
 Novikov I. D., Thorne K. S., 1973, in *Black Holes*, ed. C. De Witt & B. De Witt (New York: Gordon & Breach), 343
 Ohsuga K., Mineshige S., Mori M., Kato Y., 2009, *PASJ*, 61, L7
 Oka K., Manmoto T., 2003, *MNRAS*, 340, 543 (OM03)
 Okuda T., Molteni D., 2012, *MNRAS*, 425, 2413
 Page D. N., Thorne K. S., 1974, *ApJ*, 191, 499
 Penna R. F., McKinney J. C., Narayan R., Tchekhovskoy A., Shafee R., McClintock J. E., 2010, *MNRAS*, 408, 752
 Pohl M., 2005, *ApJ*, 626, 174
 Popham R., Gammie C. F., 1998, *ApJ*, 504, 419
 Shapiro S. L., Lightman A. P., Eardley D. M., 1976, *ApJ*, 204, 187
 Stepney S., 1983, *MNRAS*, 202, 467
 Takami H., 2011, *MNRAS*, 413, 1845
 Wu Q., Cao X., Wang D.-X., 2011, *ApJ*, 735, 50
 Wu Q., Yuan F., Cao X., 2007, *ApJ*, 669, 96
 Yuan F., 2007, in *The Central Engine of Active Galactic Nuclei*, eds. L. C. Ho and J.-M. Wang, *ASP Conference Series*, Vol. 373, p. 95
 Yuan F., Narayan R., 2013, *ARAA*, in preparation
 Yuan F., Quataert E., Narayan R., 2003, *ApJ*, 598, 301
 Yuan Y.-F., Cao X., Huang L., Shen Z.-Q., 2009, *ApJ*, 699, 722
 Xie F.-G., Yuan F., 2012, *MNRAS*, 427, 1580
 Xie F.-G., Niedźwiecki A., Zdziarski A. A., Yuan F., 2010, *MNRAS*, 403, 170
 Zdziarski A. A., Malzac J., Bednarek W., 2009, *MNRAS*, 394, L41